Structural Engineering and Mechanics, Vol. 37, No. 5 (2011) 475-487
DOI: http://dx.doi.org/10.12989/sem.2011.37.5.475

A topological optimization method for flexible multi-body dynamic system using epsilon algorithm

Zhi-Jun Yang*[1,2], Xin Chen[1] and Robert Kelly[1]

[1]*Faculty of ElectroMechanical Engineering, Guangdong University of Technology, 510006, China*
[2]*Department of Mechanical Engineering, Columbia University, New York, NY 10027, USA*

(Received December 16, 2009, Accepted October 21, 2010)

Abstract. In a flexible multi-body dynamic system the typical topological optimization method for structures cannot be directly applied, as the stiffness varies with position. In this paper, the topological optimization of the flexible multi-body dynamic system is converted into structural optimization using the equivalent static load method. First, the actual boundary conditions of the control system and the approximate stiffness curve of the mechanism are obtained from a flexible multi-body dynamical simulation. Second, the finite element models are built using the absolute nodal coordination for different positions according to the stiffness curve. For efficiency, the static reanalysis method is utilized to solve these finite element equilibrium equations. Specifically, the finite element equilibrium equations of key points in the stiffness curve are fully solved as the initial solution, and the following equilibrium equations are solved using a reanalysis method with an error controlled epsilon algorithm. In order to identify the efficiency of the elements, a non-dimensional measurement is introduced. Finally, an improved evolutional structural optimization (ESO) method is used to solve the optimization problem. The presented method is applied to the optimal design of a die bonder. The numerical results show that the presented method is practical and efficient when optimizing the design of the mechanism.

Keywords: topological optimization; the flexible multi-body dynamic system; die bonder; epsilon algorithm.

1. Introduction

The structural optimization problem has been a subject under numerous studies in recent years. Topological optimization can greatly improve the design and potential savings are generally more significant than those resulting from fixed-topology optimization (Liu and Chen 1992). It can also be used for optimal design of geometrically and materially nonlinear structures (Huang and Xie 2010), and dynamic problem with non-stochastic structural uncertainty (Lee *et al.* 2010). However, the topological optimization method is difficult to be applyed to dynamic response optimization, one of the main difficulties is the design sensitivity analysis, which is inevitable in gradient-based optimization methodology. Further difficulties involve the treatment of the dynamic constraints, and the computational solution during the optimization process.

To evaluate design sensitivity in a dynamic response optimization, one has to solve many

*Corresponding author, Ph.D., E-mail: yzj_jlu@126.com; zy2146@columbia.edu

differential equations resulting from the number of design variables and the number of active constraints (Arora 1999). If a transformation method such as the augmented Lagrangian method (ALM) is used with the adjoint variable method (AVM), the cost of calculating the design sensitivity can be reduced. However, a terminal value problem must be solved to acquire the adjoint variable for the augmented functional. If the terminal value has some error that has been accumulating over the entire time interval where the equations of motion are integrated, the adjoint variable for the augmented functional can diverge or be inaccurate. Another drawback of the ALM in dynamic response optimization is that some multiplier updating rules require the gradient of an individual response. These drawbacks reduce the attraction the ALM and AVM methods, although they considerably reduced computational effort.

Another predicament we often encounter in structural dynamic response optimization is how to treat dynamic constraints. To remove the time parameter from the dynamic constraints, it is customary to replace the dynamic constraint with an equivalent integral form or several pointwise constraints (Tseng and Arora 1989). In general, this replacement causes an increase in the number of constraints or numerical instability in the optimization procedure. We need extra effort to reduce the number of constraints or to stabilize the optimization procedure. There are many optimization examples of large structures that are subject to static loads. The existence of many practical examples means that the static response optimization methodology is well established. Design sensitivity evaluation in static response optimization does not need to solve differential equations but only simpler simultaneous algebraic equations. In the modern computing environment, it is relatively easier to solve large-scale algebraic equations. If the advantages of static response optimization can be exploited in dynamic response optimization situations, it will be much easier to perform dynamic response optimization of a structure. Basically the objective of the treatment of a dynamic constraint is the elimination of the time parameter. After eliminating the time parameter, we try to find the optimum design by using various optimization techniques. At this point, if we have some compensation for the errors of design sensitivity and response, the static response optimization process can be adopted in dynamic response optimization situations. Recently, a structural dynamic response optimization procedure using static response optimization techniques has been demonstrated (Kang *et al.* 2001, Choi and Park 2002). The main idea is transformation of a dynamic load into equivalent static loads and performing a static response optimization with the transformed equivalent static load set. This method is applied to optimization of structure with dynamic loads (Park and Kang 2003) and flexible multi-body dynamic systems (Kang *et al.* 2005). Optimization of large-scale structures using conventional formulations often involves much computational effort. Repeated solutions of the analysis and sensitivity analysis equations usually require most of this effort. The computational cost may become prohibitive in large-scale structures having complex analysis models. To alleviate this difficulty, various procedures are developed and integrated into a general optimization approach. The approach is suitable for different classes of response types and optimization methods, including linear and non-linear response (Kirsch and Bogomolni 2007, Bogomolni *et al.* 2006); static and dynamic response (Kirsch *et al.* 2006, 2007); and direct and gradient optimization methods (Kirsch *et al.* 2005). Combined approximations are used for reanalysis and repeated sensitivity analysis (Kirsch and Bogomolni 2004). The advantage is that the efficiency of local approximations and the improved quality of global approximations are combined to obtain effective solution procedures. Approximate reanalysis and finite-difference sensitivity reanalysis are considered for each intermediate design during the solution process. Reductions in the computational effort may be several orders of magnitude less than would otherwise be required. The Epsilon algorithm can accelerate the convergence speed, need less computer effort and can obtain higher accuracy even when the changes are large (Wu *et al.* 2007, Chen *et al.* 2006).

In this paper, the problem of the mechanism's structural optimization is treated as that of structural optimization using the equivalent static load method. Firstly, the actual boundary conditions of the control system and the approximate stiffness curve of the mechanism are obtained from a flexible multi-body dynamical simulation. Then according to the stiffness curve, the governing equations of the mechanism are divided into separate finite element equilibrium equations for different positions. For efficiency, the static reanalysis method is utilized to solve these equations. The detailed procedure is that, the finite element equilibrium equations of the key points in the stiffness curve are fully solved as the initial solution, and the following equilibriums are solved using a reanalysis method with the Epsilon algorithm. In order to identify the efficiency of elements, a non-dimensional measurement is introduced, and an improved ESO method is used to solve the optimization problem. The presented method is applied to the optimal design for a die bonder. The numerical results show that the method is practicable and efficient.

2. Technical background

For mechanisms operating at very high speed, the vibration of the structures must be considered, when the deformation is small, the relative nodal coordinate formulation (RNCF) with a floating frame of reference extended from the motion of the rigid body system is used Eq. (1), while for large deformations the absolute nodal coordinate formulation (ANCF) turned out to be very efficient Eq. (4).

According to previous work (Kubler 2003), the equation for the relative nodal coordinate formulation extended from the motion of the rigid body system is

$$\mathbf{M}(\mathbf{r},t)\ddot{\mathbf{r}}+\mathbf{K}(\mathbf{r},\dot{\mathbf{r}},t)+\mathbf{K}_i(\mathbf{r},\ddot{\mathbf{r}}) = \mathbf{q}(\mathbf{r},\dot{\mathbf{r}},t) \tag{1}$$

Where $\mathbf{M}(\mathbf{r},t)$ is the mass matrix of the rigid body system, $\mathbf{K}(\mathbf{r},\dot{\mathbf{r}},t)$, $\mathbf{K}_i(\mathbf{r},\ddot{\mathbf{r}})$ and $\mathbf{q}(\mathbf{r},\dot{\mathbf{r}},t)$ are the generalized elastic force, generalized Coriolis force and external force of the rigid body with position $\mathbf{r}$, respectively. The velocity and acceleration are $\dot{\mathbf{r}}$ and $\ddot{\mathbf{r}}$, respectively.

In comparison to the equation of motion of the rigid body system the additional term

$$\mathbf{K}_i(\mathbf{r},\ddot{\mathbf{r}}) = \begin{bmatrix}\mathbf{0} & \mathbf{0}\\ \mathbf{0} & \mathbf{K}\end{bmatrix}\mathbf{r}+\begin{bmatrix}\mathbf{0} & \mathbf{0}\\ \mathbf{0} & \mathbf{D}\end{bmatrix}\dot{\mathbf{r}} \tag{2}$$

depends only on the stiffness and damping matrices $\mathbf{K}$ and $\mathbf{D}$ of the flexible bodies. Moreover, the inertial matrix shows the inertial coupling due to the relative coordinates

$$\mathbf{M} = \begin{bmatrix}\mathbf{M}_{rr} & \mathbf{M}_{rf}\\ \mathbf{M}_{rf}^T & \mathbf{M}_{ff}\end{bmatrix} \tag{3}$$

where lower case r and f denote the rigid bodies and flexible body, respectively. Within ANCF for highly flexible bodies absolute coordinates are summarized in a vector $\mathbf{r}_a$ characterizing the material points of the bodies by an appropriate shape function. The equation of motion is

$$\mathbf{M}\ddot{\mathbf{r}}_a + \mathbf{K}_a(\mathbf{r}_a)\mathbf{r}_a = \mathbf{q}(\mathbf{r}_a, t) \tag{4}$$

where $\mathbf{M}$ is a constant mass matrix and the vector $\mathbf{K}_i(\mathbf{r}, \ddot{\mathbf{r}})$ of the generalized Coriolis force vanishes due to the absolute coordinates. The equation of motion for flexible bodies has the same format as structural vibration.

Using the equivalent static load method, we can derive the equivalent static load using the finite element method. The equation of the motion of a structure under a dynamic load can be written as Eq. (4), where the damping effect is ignored. Rearranging Eq. (4) yields

$$\mathbf{K}_a(\mathbf{r}_a)\mathbf{r}_a = \mathbf{q}(\mathbf{r}_a, t) - \mathbf{M}\ddot{\mathbf{r}}_a \tag{5}$$

or

$$\mathbf{K}_a(\mathbf{r}_a)\mathbf{r}_a = \mathbf{f}_{eq} \tag{6}$$

$$\mathbf{f}_{eq} = \mathbf{q}(\mathbf{r}_a, t) - \mathbf{M}\ddot{\mathbf{r}}_a \tag{7}$$

According to definition of equivalent static load method, Eq. (7) is the equivalent static load at time t.

Note that the equivalent static load can be described by the external load and inertial force. Thus the equivalent static load is an implicit function of the design variables relating to size, and even though the external force is applied to a single point of a structure, the equivalent static load is applied to all degrees of freedom of the structure.

From Eq. (7), the equivalent static load can only be obtained after performing a transient analysis of the structure to calculate the known displacement fields using an equivalent static load. From the analysis viewpoint, the equivalent static load seems to be useless. However, the goal of the equivalent static load is not to predict displacement induced by a dynamic load but to regenerate the known displacement during an optimization procedure, which will be presented in this work. In other words, the equivalent static load is not an analysis-oriented load but a design-oriented load.

The external loads and inertial forces in the FEM model can be derived from a flexible body dynamic analysis performed by ADAMS software. By using the equivalent static method, we need to build a series of structural equilibrium equations, and then the time-dependent constraint is replaced by the point wise constraints. In such cases, we need to deal with a large number of structural optimization calculations, so we introduce the fast reanalysis method to solve the sequential structural equations with a minimum of computational time. When flexible bodies move at very high speed, the inertial forces will be large and the changes to the structure would alter the performance of the structure significantly, hence the reanalysis and sensitivity analysis methods for traditional structural modification will give diverge or inaccurate results.

3. Fast solution method

Given an equivalent structure at position p with stiffness matrix $\mathbf{K}_p$ and the equivalent static load vector $\mathbf{f}_p^{eq}$, the displacements $\mathbf{r}_p$ are computed by the equilibrium equation

$$\mathbf{K}_p\mathbf{r}_p = \mathbf{f}_p^{eq} \tag{8}$$

It is assumed that the stiffness matrix $\mathbf{K}_p$ is given from the initial analysis in the decomposed form

$$\mathbf{K}_p = \mathbf{U}_p^T \mathbf{U}_p \tag{9}$$

where $\mathbf{U}_p$ is an upper triangular matrix. It is assumed that the degrees of freedom for the next position do not change, so that the finite element equation of the next position i of the structure becomes

$$\mathbf{K}_{p+i} \mathbf{r}_{p+i} = \mathbf{f}_{p+i}^{eq} \quad (i = 1, 2, \ldots) \tag{10}$$

where $\mathbf{K}_{p+i}$ is the stiffness matrix of the equivalent structure of the next ith position and vector $\mathbf{r}_{p+i}$ and $\mathbf{f}_{p+i}^{eq}$ are the corresponding displacement and load vectors.

The Eq. (10) of the equivalent structure of the next ith position can be expressed as

$$(\mathbf{K}_p + \Delta\mathbf{K}_{p+i}) \mathbf{r}_{p+i} = \mathbf{f}_p^{eq} + \Delta\mathbf{f}_{p+i}^{eq} \quad (i = 1, 2, \ldots) \tag{11}$$

where $\Delta\mathbf{K}_{p+i}$ is the increment of the stiffness matrix and $\Delta\mathbf{f}_{p+i}^{eq}$ is the increment of the equivalent static load respectively .

The goal is to find an efficient and accurate approximation of the modified displacements $\mathbf{r}_{p+i}$ due to the stiffness and equivalent static load changes in the topological modifications without solving Eq. (11). Once the displacements have been evaluated, the explicit stress-displacement relationships can readily determine the stresses

$$\boldsymbol{\sigma} = \mathbf{S}\mathbf{r} \tag{12}$$

where $\mathbf{S}$ is the stress transformation matrix.The above formulation is suitable for the whole series of equivalent static loads. The difference is only in the $\Delta\mathbf{K}_{p+i}$ term caused by the different positions due to the motion.

The perturbation method studies the system subjected to small changes in its design parameters. Therefore, if the finite element equilibrium equations of position p is represented by Eq. (10), the problem becomes that to determine $\mathbf{r}_{p+i}$ when $\mathbf{K}_p$ and $\mathbf{f}_p^{eq}$ are perturbed to the form $(\mathbf{K}_p + \Delta\mathbf{K}_{p+i})$ and $\mathbf{f}_p^{eq} + \Delta\mathbf{f}_{p+i}^{eq}$ respectively. So, the static displacement analysis problem of the perturbed system can be written as

$$\mathbf{K}\mathbf{r} = \mathbf{f} \tag{13}$$

where

$$\mathbf{K} = \mathbf{K}_p + \Delta\mathbf{K}_{p+i} \tag{14}$$

$$\mathbf{f} = \mathbf{f}_p^{eq} + \Delta\mathbf{f}_{p+i}^{eq} \tag{15}$$

$$\mathbf{r} = \mathbf{r}_0 + \varepsilon\mathbf{r}_1 + \varepsilon^2\mathbf{r}_2 + \varepsilon^3\mathbf{r}_3 + \ldots \tag{16}$$

Substituting Eqs. (14), (15) into Eq. (13),we can get

$$\mathbf{r}_0 = \mathbf{K}_p^{-1} \mathbf{f}_p^{eq} \tag{17}$$

$$\mathbf{r}_1 = \mathbf{K}_p^{-1} (\Delta\mathbf{f}_{p+i}^{e} - \Delta\mathbf{K}_{p+i} \mathbf{r}_0) \tag{18}$$

$$\mathbf{r}_2 = -\mathbf{K}_p^{-1} \Delta\mathbf{K}_{p+i} \mathbf{f}_1 \tag{19}$$

$$\ldots.$$

$$\mathbf{r}_s = -\mathbf{K}_p^{-1}\Delta\mathbf{K}_{p+i}\mathbf{f}_{s-1} \quad (s = 2, 3, 4, \ldots) \tag{20}$$

If we consider an infinite sequence $\{\mathbf{r}_0, \mathbf{r}_1, \mathbf{r}_2, \ldots\}$, and let the $\mathbf{s}_n$ be the partial sum of the sequence, then we have a new sequence $\{\mathbf{s}_0, \mathbf{s}_1, \mathbf{s}_2, \ldots\}$

$$\mathbf{s}_n = \sum_{i=0}^{n}\mathbf{r}_i \quad n = 0, 1, 2, \ldots \tag{21}$$

$$\mathbf{s} = \lim_{n\to\infty}\mathbf{s}_n \tag{22}$$

For the sequence $\{\mathbf{s}_0, \mathbf{s}_1, \mathbf{s}_2, \ldots\}$, we construct an iterative form

$$\boldsymbol{\varepsilon}_{-1}^{(j)} = \mathbf{0} \tag{23}$$

$$\boldsymbol{\varepsilon}_0^{(j)} = \mathbf{s}_j \tag{24}$$

$$\boldsymbol{\varepsilon}_{k+1}^{(j)} = \boldsymbol{\varepsilon}_{k-1}^{(j+1)} + [\boldsymbol{\varepsilon}_k^{(j+1)} - \boldsymbol{\varepsilon}_k^{(j)}]^{-1}, \quad j = 0, 1, \ldots, \; k = 0, j-1 \tag{25}$$

The iteration formula (23)-(25) is similar to the scalar case (Wu *et al.* 2007), and the inverse of a vector $\boldsymbol{\varepsilon}^{-1}$ defined as

$$\boldsymbol{\varepsilon}^{-1} = \frac{\boldsymbol{\varepsilon}^*}{(\boldsymbol{\varepsilon}^H\boldsymbol{\varepsilon})} = \frac{\boldsymbol{\varepsilon}^*}{\sum_{i=1}^{d}\varepsilon_i^2} \tag{26}$$

where the asterisk denotes the complex conjugate and H the Hermitian conjugate. The vector epsilon-algorithm table can be also constructed by Eqs. (8)-(10).

In order to control the accuracy of the Epsilon Algorithm for a vector series, an error value is given to assure the demand of better kinematic and dynamic performance of a high-speed mechanism is met. The error e_R is evaluated by

$$e_R = 100\frac{\left\|\varepsilon_k^{(0)} - \varepsilon_{k-2}^{(0)}\right\|}{\left\|\varepsilon_k^{(0)}\right\|} < T \tag{27}$$

where T is the given tolerance. If sufficient accuracy is not achieved, then increasing the number of iterations j will result in more computational cost. The maximum number of iterations is controlled by the user. If the maximum iterative number is reached and no solution is achieved within the tolerances required then the specific equations cannot be solved by the reanalysis method. In this situation, a full solution is required to solve this equation and thus becomes the new original solution for the next equivalent static load of the structure. Fig. 1 shows how the reanalysis method is performed in the mechanism system. p_i^0 is the location where a full solution must be performed, and the next few structural dynamic equations can be solved using the reanalysis method just mentioned. The interval between equations can be determined by the rate of change of the stiffness of the system. The number of reanalysis points can be set in advance or interactively during the solution.

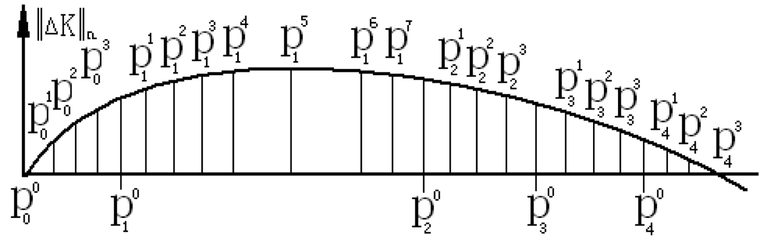

Fig. 1 Indication of solution of serial equivalent static load equations using the reanalysis method

4. Sensitivity analysis

To identify the efficiency of the material, the element sensitivity of the strain energy of elements is introduced. Suppose that an element is removed from the base structure, the element sensitivity of the strain energy is defined by

$$\Delta E_i = E_i^e = \frac{1}{2}\mathbf{r}_i^T\mathbf{K}_i^e\mathbf{r}_i \tag{28}$$

where $\mathbf{K}_i^e$ is the stiffness matrix of the i^{th} element of the structure, $\mathbf{r}_i$ is the displacement vector of the i^{th} element, and E_i is used to denote the element sensitivity of the strain energy as the result of removing the i^{th} element from the reference structure. Using Eq. (28) the all element sensitivity of strain energy of the structures, $(i = 1, 2, \ldots, n)$, can be obtained. We then define

$$s_i = \frac{1}{c}\sum_{j=1}^{c} E_{i,j}^e/\max(E_{1,j}^e, E_{2,j}^e, \ldots, E_{n,j}^e) \tag{29}$$

where n is the number of the optimable elements , c is the number of loadcases, $\max(E_{i,j}, E_{2,j}, \ldots. E_{n,j})$ is the maximum element of the j^{th} loadcase; s_i are the non-dimensional measures for identification of those elements of the structures which need to be kept or removed. Then the criterion for determining the efficiency of material is defined as follows

$$s_i \geq s_k^* \tag{30}$$

where s_k^* is a threshold value for determining the efficiency of material at k^{th} iteration. If the search criterion, Eq. (30), is satisfied, the i^{th} element of the structures can be retained; otherwise the i^{th} element should be removed.

5. The topological optimization procedure

In the topological optimization of a mechanism's structures, the objective is to find the optimal topology and configuration of material, which minimizes the weight of the structures within global stiffness constraints.The total strain energy is used as the inverse measurement of the global stiffness of the structure. Thus the layout optimization problem of structures can be formulated as follows

$$
\begin{aligned}
& Min \quad M \\
& s.t. \quad E \le E^*
\end{aligned} \tag{31}
$$

where M is the total mass of the structure, and E^* is a given threshold value, E is the total strain energy of the structure given by

$$E = \frac{1}{2}\mathbf{r}^T\mathbf{K}\mathbf{r} = \frac{1}{2}\mathbf{f}^T\mathbf{r} \tag{32}$$

where $\mathbf{K}$ is the stiffness matrix of the structure, $\mathbf{f}$ and $\mathbf{r}$ are the load and displacement vectors, respectively.

The procedure of the topological optimization of mechanism's structures is given as follows.

Step1. Carry out the dynamic analysis of the flexible multibody system, obtain the velocity and acceleration for any position, and export as the load case for each equivalent structural dynamic response.

Step2. Build finite element models for each position of the motion using the exported boundary condition and formulate a series of static equilibrium equations.

Step3. Solve the static equilibrium equations using the reanalysis method presented by this paper.

Step4. Calculate the element sensitivity with regard to the strain energy of each equivalent structure using Eq. (28), and combine all of the element sensitivity results using Eq. (29).

Step5. Use the search criterion Eq. (30) to decide which elements need to be kept or removed. At the k^{th} iteration, the threshold value s_k^* is determined by

$$s_k^* = s_k^0 + \Delta s_k \tag{33}$$

With this increased rejection threshold value, the elements of the structures can be removed repeatedly until the optimal structures are obtained. The elements are defined as special material instead of being deleted immediately. Therefore, the removed elements can be recovered in later iterations. The procedure requires two parameters to be prescribed. The first is the initial rejection ratio s_k^0 and the second is the increased rate Δs_k^i. Values of $s_k^0 = 0.01$ and $\Delta s_k = 0.005$ have been used for many test examples.

Step6. Update the displacements and element strain energy of structures using the error controlled Epsilon algorithm.

Step7. Evaluate the total strain energy E of the structure. Repeat steps 4-6 until the following condition is no longer satisfied, the optimal layout of structures is obtained

$$E \le E^* \tag{34}$$

or the following condition is satisfied, the the layout optimization of structures is also considered to be obtained.

$$\Delta M < \varepsilon \tag{35}$$

where M is the mass of removed structures at k^{th} iteration, and $\mathring{a}$ is a given small value.

Step8. Remove the elements by deleting material from the final result, and smooth the boundary using a smoothing method such as the OOsmooth software in Hyperworks.

6. Numerical example

During the operation of a die bonder, the bonder (Fig. 2) moves on to the wafer and picks up a die, and then moves back and bonds it onto the leadframe. As the capillary moves at very high speeds, it is necessary to optimally design the mechanism so as to obtain the best dynamic performance. The assembly model of the die bonder with the arm at a 90º drive angle is shown in Fig. 2 and the corresponding assembly finite element model is shown in Fig. 3. The finite element of the arm of the die bonder includes 23153 solid elements and 25744 nodes. The material of structures is aluminum with Young's modulus 71.75 GPa and mass density 2740 kg/m^3. During the

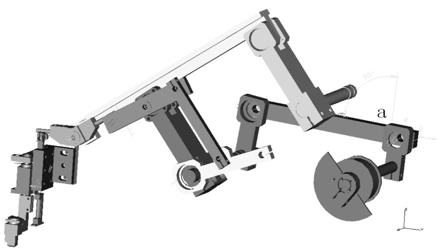

Fig. 2 Assembly of the die bonder

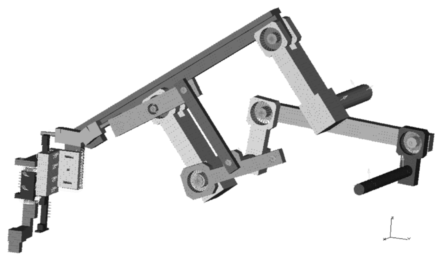

Fig. 3 Finite element Model of the die bonder

Table 1 Frequencies of the first ten modes of the die bonder in different position

α (º)	Mode1 Freq(Hz)	Mode 2 Freq(Hz)	Mode 3 Freq(Hz)	Mode 4 Freq(Hz)	Mode 5 Freq(Hz)	Mode 6 Freq(Hz)	Mode 7 Freq(Hz)	Mode 8 Freq(Hz)	Mode 9 Freq(Hz)	Mode 10 Freq(Hz)
0	0.039	112.6832	117.7509	221.7676	232.284	396.1588	510.8086	629.2661	728.7595	884.9595
10	0.045	112.6861	185.1197	221.2857	234.6903	396.5793	510.5535	629.742	728.8834	884.1193
20	0.027	112.699	218.9099	227.4708	298.0035	398.4157	509.8322	631.1407	729.0269	880.8168
30	0.088	112.733	216.0793	228.8021	370.9492	409.0406	509.0369	633.3381	729.333	875.4335
40	0.175	112.8015	212.3618	229.1991	388.5817	448.9342	508.9621	636.1638	730.0094	868.7857
50	0.264	112.9155	208.2248	229.6411	390.5916	481.3221	511.8741	639.4336	731.2723	861.8146
60	0.342	113.0796	203.9979	230.3455	390.6403	494.6158	521.8949	642.9725	733.3023	855.3318
70	0.412	113.2918	199.9167	231.436	390.0111	497.7388	533.0556	646.6244	736.2223	849.9092
80	0.473	113.5424	196.1336	232.9899	389.0336	498.707	539.4266	650.2569	740.0904	845.8785
90	0.528	113.8166	192.7367	235.0379	387.8753	499.1963	540.3386	653.7616	744.914	843.3852
100	0.584	114.0953	189.7678	237.5547	386.6549	499.2882	535.9728	657.0528	750.6514	842.4299
110	0.64	114.3593	187.2372	240.4532	385.4669	498.0139	526.9898	660.0629	757.186	842.8739
120	0.703	114.5904	185.1348	243.5729	384.3826	490.8803	516.9234	662.7319	764.2741	844.4258
130	0.771	114.7728	183.4375	246.6675	383.4332	469.3288	512.4347	665.004	771.5254	846.682
140	0.838	114.8909	182.115	249.3502	382.4955	431.9569	511.8312	666.8307	778.4422	849.2025
150	0.894	114.9172	181.1338	250.7785	372.7502	385.9856	512.2935	668.1843	784.5007	851.5892
160	0.914	114.749	180.4611	245.8238	303.2969	382.8814	512.9369	669.0674	789.2372	853.5415
170	0.805	113.6145	180.0518	185.6277	266.3805	382.5668	513.4389	669.5137	792.3149	854.8826
180	0.039	104.3495	129.7162	179.9479	263.5894	382.4923	513.671	669.5726	793.5544	855.5465

motion, the drive angle changes from 0 to 180 degrees. From the modal analysis at different positions, it can be seen that the natural resonance frequencies vary with drive angle (Table 1).

The frequencies of the first ten modes of all positions (with drive angle increments of 10 degrees) are listed in Table 1, and the frequency vs. drive angle for the first ten modes are shown in Fig. 4. These results show that the first mode is rigid motion, and modes 3-7 are more sensitive to drive angle.

In order to reduce the mass of the die bonder such that the inertial force can be reduced, the component structures of the die bonder arm are optimized using the presented methods.The frequencies of the first ten flexible modes during the process of optimization are listed in the Table 2.

In the first iteration, 1334 elements at low sensitivity are modified; note that the rate of change for each component is different. In the second iteration, the material of all the elements are reassigned according to the combined sensitivity, 2050 elements are defined as deleted material, and Young's

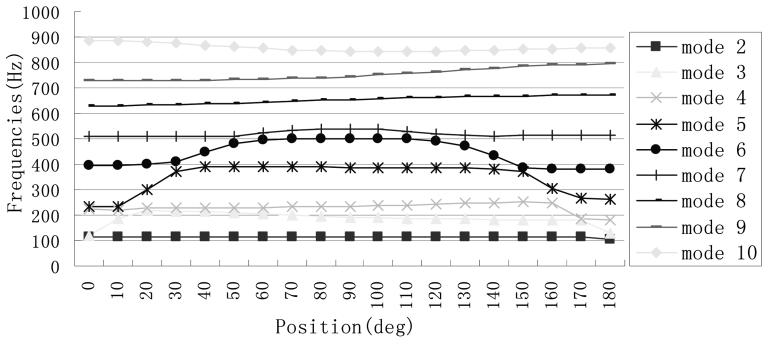

Fig. 4 Frequency vs. drive angle for the first ten modes

Table 2 The frequencies of the first ten modes of the specific position during optimal design

mode		Frequencies of structures (Hz)				Change	Rate of Change
		Original	Step1	Step2	Step3		
2		119.6361	118.2105	120.276	119.8268	0.1907	0.16%
3		204.2693	206.3296	202.1958	198.1035	-6.1658	-3.02%
4		247.507	252.7171	240.7929	237.5691	-9.9379	-4.02%
5		328.2244	396.2702	323.9933	315.9957	-12.2287	-3.73%
6		452.7336	498.1879	465.587	465.7856	13.052	2.88%
7		492.8783	623.4556	487.9892	483.922	-8.9563	-1.82%
8		623.8224	786.0137	610.6964	598.4155	-25.4069	-4.07%
9		734.9551	993.0482	744.2667	742.308	7.3529	1.00%
10		928.4488	1099.8681	919.6725	918.7554	-9.6934	-1.04%
11		1069.6187	1132.44	1097.703	1106.515	36.8963	3.45%
Mass (kg)	Total	0.5602	0.5263	0.5029	0.4876	-0.0726	-12.96%
	Optimable Structures	0.3378	0.3035	0.2799	0.2652	-0.0726	-21.49%
Deleting Elements		0	1334	2050	2591	2591	11.19%

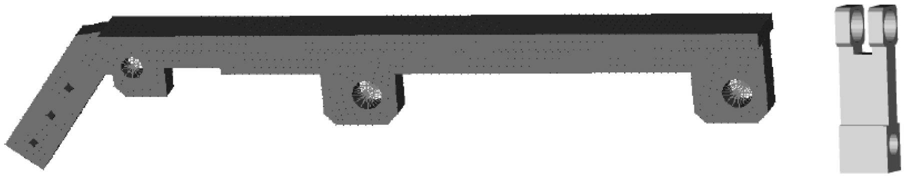

Fig. 5 Original structure of Link 5 and crank 3 of the die bonder

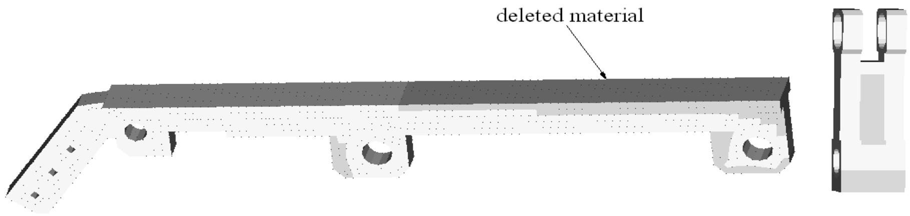

Fig. 6 Removing elements of structures Link 5 and crank 3 of the die bonder

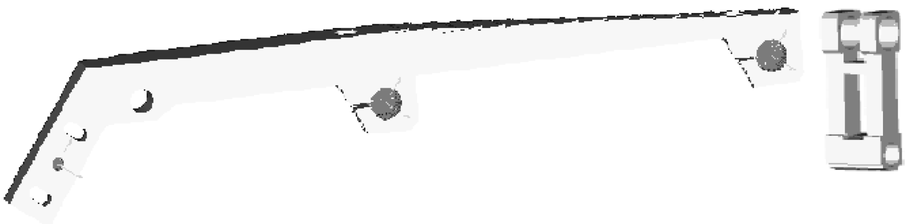

Fig. 7 Optimal structure of Link 5 and crank 3 of the die bonder

Table 3 The comparison of residual vibration and drive torque

	Residual vibration		Drive Torque	
	Magnitude (μm)	Change Rate (%)	Magnitude (N·mm)	Change Rate (%)
Base	35.4820	-	834.9584	-
Optimal	28.4600	-19.7903	672.1309	-19.5013

modulus and mass density are within 1% of the normal material (Fig. 6). In the final optimal design where the elements are completely removed (Fig. 7), the frequencies of the vibration are changed very little, but the mass of the structure is reduced 21.49%. These results show that the presented approach is efficient and easy to carry out.

In order to show the efficiency of optimization, the residual vibration (Fig. 8) and drive torque (Fig. 9) are compared between the base structure and the optimal structure obtained by the presented method. Note that the base structure is the most stiffener structure of the possible design space. It can be seen (shown in Table 3) that the maximum residual vibration magnitude is smaller (decreased 19.7903%) but nearly the same due to the stiffness constraints. Meanwhile, the drive torque became smaller due to the reduced mass thus needing less power (reduced 19.5013%) for the same motion profile of the die bonder.

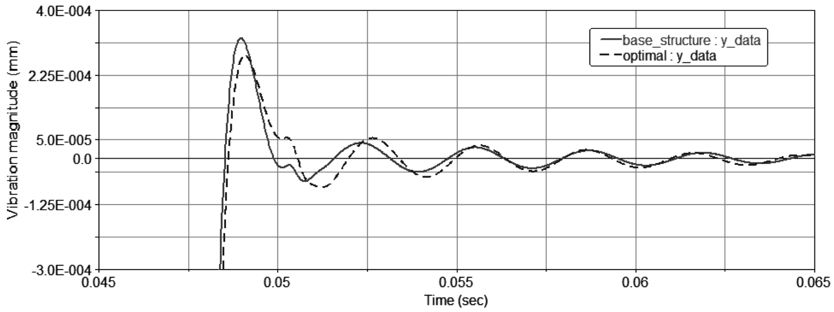

Fig. 8 The residual vibration magnitude curve

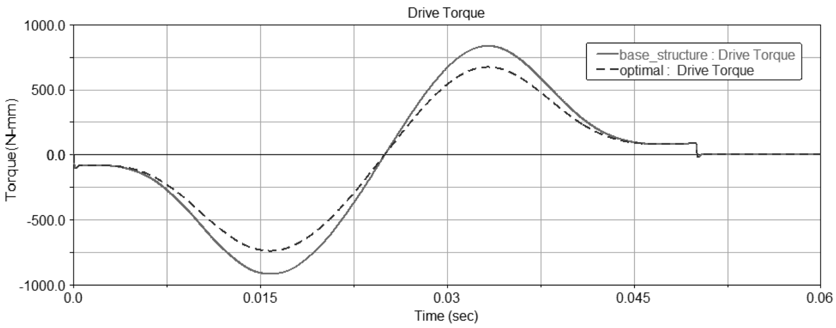

Fig. 9 The driven torque curve

7. Conclusions

In this paper, a topological optimization method for flexible multi-body dynamic system has been presented. In this process, the actual boundary conditions of the control system and the approximate stiffness curve of mechanism are calculated from a flexible multi-body dynamics simulation, and the governing equations of the mechanism are divided into separated finite element equilibrium equations for different positions according to the stiffness curve. For efficiency, the static reanalysis method is utilized to solve these equations, a non-dimensional measurement is introduced to identify the efficiency of the elements, and an improved ESO method is used to solve the optimal design problem. The presented method is easy to implement with a general finite element system and convenient to use in various engineering problems. The present method was implemented for the topological optimization of a die bonder. From the example shown in Table 2, it can be seen that only three iterations were needed for obtaining the optimal configuration of material. The flexible multibody simulation shows that the residual vibration can be restrained by stiffness constraints, and the driven power can be minimized due to the lower inertial force using an updated lightweight design.

Acknowledgements

This research has been supported by the National Science Foundation for Young Scientists of

China (Grant No. 50905033), the Specialized Research Fund for the Doctoral Program of Higher Education of China (Grant No. 20094420120001), the National Science Foundation for Post-doctoral Scientists of China (Grant No.20094420120001), Guangdong Natural Science Foundation (845100900100414), the Post-doctoral Science Foundation of China (Grant No.20070420761), the Guangdong Provincial Science Plan Project (Grant No.2009B010900032); the Produce-learn-research project of Zhongshan City (Grant No. 2009CXY018). In addition, we would like to thank John P. Hilton (Department of Mechanical Engineering, Columbia University) for the help in revising the language in this manuscript.

References

Arora, J.S. (1999), "Optimization of structures subjected to dynamic loads. structural dynamic systems", *Comput. Tech. Opt.*, **7**, 1-73.

Bogomolni, M., Kirsch, U. and Sheinman, I. (2006), "Nonlinear dynamic sensitivities of structures using combined approximations", *AIAA J.*, **44**(11), 2765-2772.

Chen, S.H., Wu, X.M. and Yang, Z.J. (2006), "Eigensolution reanalysis of modified structures using epsilon-algorithm", *Int. J. Numer. Meth. Eng.*, **66**(13), 2115-2130.

Choi, W.S. and Park, G.J. (2002), "Structural optimization using equivalent static loads at all the time intervals", *Comput. Meth. Appl. Mech. E.*, **191**(19-20), 2105-2122.

Huang, X. and Xie, Y.M. (2010), "Evolutionary topology optimization of geometrically and materially nonlinear structures under prescribed design load", *Struct. Eng. Mech.*, **34**(5), 581-595.

Kang, B.S., Choi, W.S. and Park, G.J. (2001), "Structural optimization under equivalent static loads transformed from dynamic loads based on displacement", *Comput. Struct.*, **79**(2), 145-154.

Kang, B.S., Park, G.J. and Arora, J.S. (2005), "Optimization of flexible multibody dynamic systems using the equivalent static load method", *AIAA J.*, **43**(4), 846-852.

Kirsch, U., Bogomolni, M. and Sheinman, I. (2007), "Efficient dynamic reanalysis of structures", *J. Struct. Eng.-ASCE*, **133**(3), 440-448.

Kirsch, U. and Bogomolni, M. (2004), "Procedures for approximate eigenproblem reanalysis of structures", *Int. J. Numer. Meth. E.*, **60**(12), 1969-1986.

Kirsch, U. and Bogomolni, M. (2007), "Nonlinear and dynamic structural analysis using combined approximations", *Comput. Struct.,* **85**(10), 566-578.

Kirsch, U., Bogomolni, M. and Sheinman, I. (2006), "Efficient procedures for repeated calculations of the structural response using combined approximations", *Struct. Multidiscip. O.*, **32**(6), 435-446.

Kirsch, U., Bogomolni, M. and van Keulen, F. (2005), "Efficient finite difference design sensitivities", *AIAA J.*, **43**(2), 399-405.

Kubler, L., Eberhard, P. and Geisler, J. (2003), "Flexible multibody systems with large deformations and nonlinear structural damping using absolute nodal coordinates", *Nonlinear Dynam*, **34**(1-2), 31-52.

Lee, D.K., Starossek, U. and Shin, S.M. (2010), "Topological optimized design considering dynamic problem with non-stochastic structural uncertainty", *Struct. Eng. Mech.*, **36**(1), 79-94.

Liu, Z.S. and Chen, S.H. (1992), "Reanalysis of static response and its design sensitivity of locally modified structures", *Commun. Numer. Meth. En.,* **8**, 797-800.

Park, G.J. and Kang, B.S. (2003), "Validation of a structural optimization algorithm transforming dynamic loads into equivalent static loads", *J. Optimiz. Theory App.*, **119**(1), 191-200.

Tseng, C.H. and Arora, J.S. (1989), "Optimum design of systems for dynamics and controls using sequential quadratic programming", *AIAA J.*, **27**(12), 1793-1800.

Wu, X.M., Chen, S.H. and Yang, Z.J. (2007), "Static displacement reanalysis of modified structures using the epsilon algorithm", *AIAA J.,* **45**(8) 2083-2086.